



# A Comparative Study between 2-D Method and Ferrari Method to Control Torque of IPMSM

Gopal S M.E<sup>1</sup>, Shanmugapriya P M.E<sup>2</sup>

Dept. of Electrical and Electronics Engineering, Sri Sairam Engineering College, Chennai, India<sup>1,2</sup>

**Abstract**—For the torque control of an interior permanent magnet synchronous motor (IPMSM), it is necessary to determine a current command set that minimizes the magnitude of the current vector. This is known as the maximum torque per ampere. In the field-weakening region, current minimizing solutions are found at the intersection with the voltage limits. However, the optimal problem yields fourth-order polynomials (quartic equations), and no attempt has been made to solve these quartic equations online for torque control. Instead, premade lookup tables are widely used. These lookup tables tend to be huge because it is necessary to create separate tables on the basis of the dc-link voltage and motor temperature. In this study, we utilize Ferrari's method, which gives the solution to a quartic equation, for the torque control. Further, a recursive method is also considered to incorporate the inductance change from the core saturation. A simulation and some experiments were performed using an electric vehicle motor, which demonstrated the validity of the proposed method.

**Index Terms**—Electric vehicle (EV), Ferrari's method, interior permanent magnet synchronous motor (IPMSM), maximum torque per ampere (MTPA), torque control, voltage limit.

## I. INTRODUCTION

AN interior permanent magnet synchronous motor (IPMSM) is known to be a superior solution in terms of efficiency, power density, and wide speed operating range. Because the reluctance torque can be utilized in the field-weakening region, the speed range of an IPMSM can be extended while maintaining a constant power. This wide constant-power speed range gives the

virtue of high power density. In an IPMSM, the torque is determined using not only the  $q$ -axis current  $i_q$ , but also the  $d$ -axis current  $i_d$ . Therefore, there has been a question of optimality in combining the two current components. The solution is to produce the desired torque while minimizing the current magnitude. The maximum torque per ampere (MTPA), developed by Morimoto *et al.*, is the current minimizing solution that is used under the base speed. Above the base speed, the MTPA is not feasible because of the limit in the dc-link voltage. In general, the optimal combination is found at the intersection of the torque and voltage limit curves. There are two problems that hinder pursuing the optimality in a practical situation: finding the intersection of the two curves is a highly nonlinear problem and the inductances change along with the current as a result of core saturation. Even cross-coupling phenomena cannot be neglected in some specific applications.

Thus, lookup table methods are widely used in the IPMSM torque control. They calculate the optimal current commands *a priori*, put them into a table, and then draw current commands from this table on the basis of the required torque and speed.

Nalepa and Kowalska effectively demonstrated the difficulty in finding the optimal solution owing to magnetic saturation and temperature variations. They proposed the use of a 3-D table in generating a feed-forward compensation term for the  $d$ -axis current command based on the dc-link voltage,  $q$ -axis current, and speed. It should be noted that the field strength of a permanent magnet, for example a neodymium magnet, depends on the temperature, and its change cannot be neglected in electric vehicle (EV) applications because the ambient temperature is in the range of  $-40$ – $150$  °C. Monajemy and Krishnan derived a fourth-order



polynomial that resulted from torque and voltage limit equations and proposed the use of solution lookup tables based on flux linkage and torque commands.

Instead of using the lookup table, analytic approaches based on the mathematical model were attempted. However, those approaches were limited in practical use, because no explicit current set was obtainable from a given desired torque. Jeong *et al.* formulated current cost functions with torque and voltage constraints, and proposed the use of Newton's method online to find the minimizing solutions. However, the convergence and computational burden would be problematic in real-time applications. Lee *et al.* Separated the cases on the basis of whether or not the solution was within the voltage limit and derived fourth-order polynomials in both cases. They found solutions by using a technique of approximating the fourth-order polynomial by a second-order one. Bolognani proposed a local MTPA search method involving the injection of an additional pulsating current. Based on the magnitude of torque ripple, they constructed an MTPA-tracking loop. The torque ripple was measured indirectly via speed variation in the experiment

Direct torque control (DTC) for IPMSM drives has been investigated since the 1990s. DTC does not require an accurate motor model and parameters, except for the armature resistance. The torque and stator flux linkage are directly controlled using both a hysteresis comparator and a switching table [14], [15]. However, there are problems, such as an unfixed switching frequency and a large torque ripple. To solve these problems, space vector modulation was used, along with a reference flux vector calculator (RFVC) [16]. Relevant DTC methods that considered the voltage and current limits were followed.

For a surface-mounted permanent magnet synchronous motor (SPMSM), selecting the optimal current set is simpler than for an IPMSM. Chen *et al.* [19] proposed a current controller for an SPMSM that adjusted the  $d$ -axis current on the basis of the voltage saturation. Because the current set was found on the voltage boundary, it was claimed to be optimal in the sense of minimizing the copper loss. Liu *et al.* [20] proposed an improved method of tracking the maximum torque per voltage line in an SPMSM by including the stator resistance and inverter nonlinearities.

In this paper, an online torque control method based on analytic solutions is proposed that covers the entire speed region. Fourth-order polynomials are derived from the optimality conditions. Two optimality conditions are considered: within the base speed region and in the field-weakening region where the voltage limits is active. A discriminant is used to discern these two cases. Ferrari's method is used to find the solution of quartic equations.

Through repeating the computations, variations in the  $d$  and  $q$ -axes inductances are considered. This paper is organized as follows. Section II provides preliminaries on the IPMSM model, inductance saturation effect, and motor losses. In Section III, current minimizing conditions are derived with and without the voltage limit. Then, Ferrari's method is used to solve quartic polynomials in Section IV, and a current minimizing algorithm is proposed in Section V. The entire torque control algorithm is constructed in Section VI. Finally, a simulation and some experiments are shown in Sections VII and VIII.

## II. PRELIMINARIES

### A. IPMSM Model and Voltage/Current Limits

Fig. 1 shows a 2-D FEM model of an IPMSM used in this experiment. The motor was developed as a propulsion motor for C-class passenger EVs. The outer diameters of stator and rotor are 249 and 171 mm, respectively. The stack length is 120 mm and the air-gap height is 0.8 mm. It has eight poles and two permanent magnets are arranged in a v-shape in each pole. Cavities were designed around the edges of permanent magnets to reduce the leakage flux.

Considering core saturation effects, the stator flux linkage of the IPMSM in the synchronous reference frame is described by

$$\lambda_d = L_d(i_d, i_q)i_d + \psi_m \quad (1)$$

$$\lambda_q = L_q(i_d, i_q)i_q \quad (2)$$

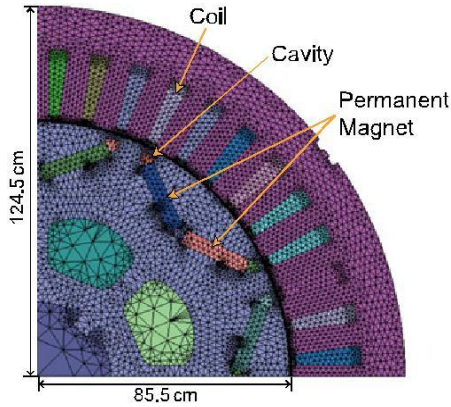


Fig. 1. 2-D mesh model of the IPMSM.

where  $i_d$  and  $i_q$  are the  $d$ - and  $q$ -axes currents;  $L_d$  and  $L_q$  are the  $d$ - and  $q$ -axes inductances; and  $\psi_m$  is the rotor flux linkage due to the permanent magnets.

The stator voltage equations of the IPMSM in the synchronous frame are

$$v_d = r_s i_d + L_d \frac{di_d}{dt} - \omega_e L_q i_q \quad (3)$$

$$v_q = r_s i_q + L_q \frac{di_q}{dt} + \omega_e L_d i_d + \omega_e \psi_m \quad (4)$$

where  $v_d$  and  $v_q$  are the  $d$ - and  $q$ -axes voltages;  $\omega_e$  is the electrical angular frequency; and  $r_s$  is the stator resistance. The electromagnetic torque equation of the IPMSM is given by

$$T = \frac{3}{4} P (\psi_m i_q + (L_d - L_q) i_d i_q) \quad (5)$$

(5) where  $P$  is the pole number.

Neglecting the ohmic drop across the stator resistance, the current and voltage limits are described by

$$i_d^2 + i_q^2 \leq I_s^2 \quad (6)$$

$$L_d^2 \left( i_d + \frac{\psi_m}{L_d} \right)^2 + L_q^2 i_q^2 \leq \frac{V_s^2}{\omega_e^2} \quad (7)$$

where  $I_s$  is the peak value of the maximum stator current and  $V_s$  is the peak value of the maximum phase voltage.

As shown in Fig. 2, the current limit is the dashed circle centered at the origin with radius  $I_s$ . The voltage limit appear as the dotted ellipse centered at  $(-\psi_m/L_d, 0)$ , and the major and minor radii are  $V_s/(L_d \omega_e)$  and  $V_s/(L_q \omega_e)$ , respectively. Therefore, the voltage limit ellipse shrinks as  $\omega_e$  increases.

### B. Inductance Change Due to the Core Saturation

In most torque control applications, torque sensors are not used directly. Instead, torque estimates based on the stator current measurements are used for feedback. Therefore, accurate inductance information is indispensable for a better torque precision and for an optimal current command selection. However, due to the core saturation, the inductances vary nonlinearly depending on the load condition and current

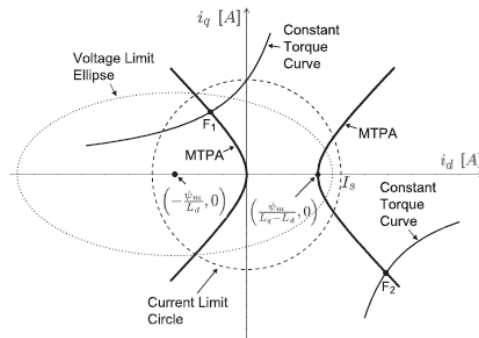


Fig. 2. Current limit circle, voltage limit ellipse, and constant torque curve on  $d$ - $q$  axes.

$$fd(i_d, i_q) = r_s i_d - \omega_e L_q(i_d, i_q) i_q \quad (8)$$

$$fq(i_d, i_q) = r_s i_q + \omega_e L_d(i_d, i_q) i_d + \omega_e \psi_m \quad (9)$$

Specifically, we measure the  $d$ - and  $q$ -axes voltages two times in the steady state, altering the polarity of the  $q$ -axis current, we measure  $fd(i_d, i_q)$ ,  $fd(i_d, -i_q)$  and  $fq(i_d, i_q)$

),  $f_q(i_d, -i_q)$  under regulated current conditions, and estimate inductances in,

$$L_d(i_d, i_q) = \frac{f_q(i_d, i_q) + f_q(i_d, -i_q) - 2\omega_e \psi_m}{2\omega_e i_d} \quad (10)$$

$$L_q(i_d, i_q) = \frac{f_d(i_d, -i_q) - f_d(i_d, i_q)}{2\omega_e i_q} \quad (11)$$

### C. Motor Losses

The losses of motor consist of copper loss, iron loss, stray loss, and mechanical loss. The copper loss refers to the joule loss of the stator coil, and is described by

$$P_{cu} = \frac{3}{2} r_s (i_d^2 + i_q^2) \quad (12)$$

In the extreme high speed range, the iron loss grows significantly. However, it is still smaller than the copper loss.

The mechanical and stray losses are small compared with the copper and iron losses. Fig. 5 shows copper and iron loss of the IPMSM used in this experiment

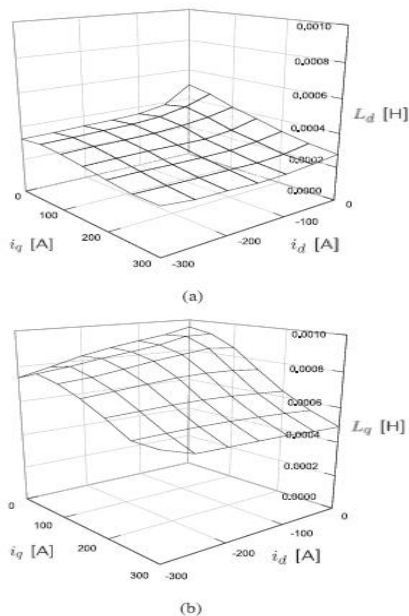


Fig. 3. Variations in  $L_d$  and  $L_q$  depending on currents. (a)  $L_d$ . (b)  $L_q$ .

To estimate inductances, we use voltage measurements. To estimate inductances, we use voltage measurements. The iron loss means the loss of the iron core for a time-varying field. It consists of two parts: hysteresis loss and eddy current loss. Since the loop area of a  $B-H$  curve signifies an energy per volume, the hysteresis loss is proportional to the frequency and the loop area. The loop area does not grow linearly with the maximum field  $B_m$ . Experimentally, it is estimated by  $khfB_m^\alpha$  where  $kh = 40-55$  is a constant depending on the silicon contents in the steel,  $f$  is a frequency of the field, and  $\alpha$  is in the range of 1.8-2.2 [22]. The latter is often called Joule loss, since it is caused by induced current in the conductive magnetic material. It is predicted analytically by  $kef^2B_m^2$ , where  $ke$  is a constant which depends on the thickness of the steel lamination and the silicon percentage. Putting together, the iron loss under sinusoidal excitation is model

$$P_{Fe} = k_h f B_m^\alpha + k_e f^2 B_m^2 \quad (13)$$

. The iron losses were calculated over a wide speed range under various current conditions using a commercial FEM tool, JMAG. The results state that copper loss is most dominant especially in the low-speed area.

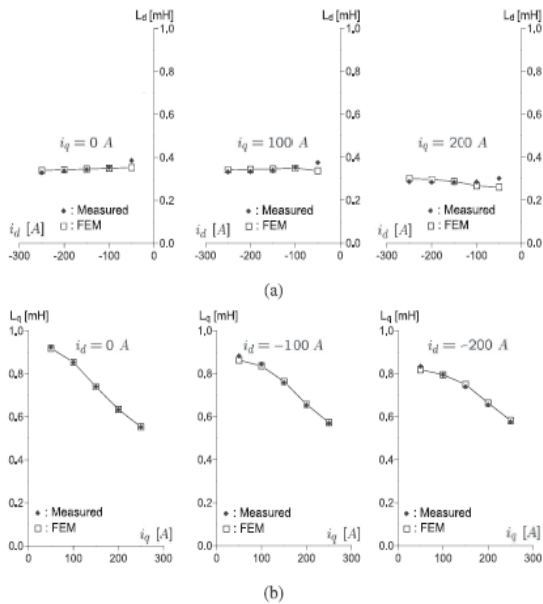


Fig. 4. Inductance comparison between measured and FEM data: (a)  $L_d$  and (b)  $L_q$ .

Numerous research works were performed regarding the total loss minimization of an IPMSM. Morimoto et al. established a loss minimizing control based on an equivalent circuit which contained an iron loss model as well as a copper loss model. Utilizing a derivative of the loss function, a loss-minimizing d-axis current was determined. Cavallaro et al. developed an online loss minimizing algorithm based on the loss model of Morimoto. Lee et al. proposed a method of finding the loss minimizing solution using an approximation technique.

The total loss minimization is not an easy task because a target cost function itself is a high-order polynomial if an iron loss model is included. Furthermore, the coefficients vary depending on current and frequency [25]. Thereby, an explicit form of analytical solutions is hardly obtainable. Furthermore, the computational load should not be high for practical applications. In this study, we narrow down the focus to the copper loss minimization like the MTPA. But we consider voltage and current limits, while accepting inductance variations.

### III. ANALYTIC SOLUTION FOR CURRENT MINIMIZATION

In order to establish a torque control loop, it is necessary to find the current command values,  $(i_d^*, i_q^*)$ .

There are numerous  $(i_d, i_q)$  choices for a given torque, as shown in Fig. 2. However, each choice needs to be evaluated from the perspective of loss minimization. It should be noted that the winding copper loss is the dominant one among many loss components. Thus, a simple optimization method is to focus on just reducing the stator current, and the MTPA is such a current minimizing solution.

If a torque curve intersects the MTPA line within the voltage and current limits, then the intersection point will be a desired current command. However, the MTPA solution may be located outside the voltage limit, as shown in Fig. 6. In such cases, a suboptimal solution is found at the intersection between the torque curve and the voltage limit ellipse.

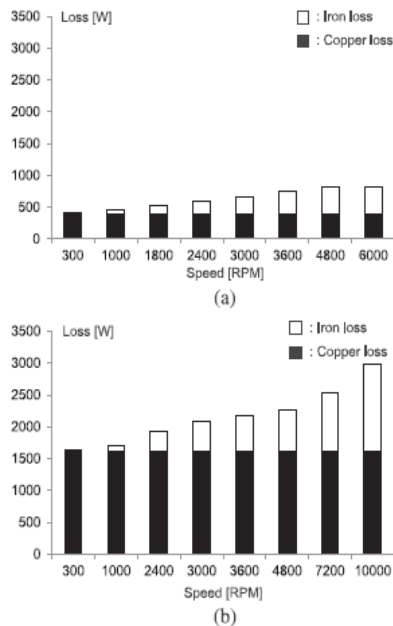
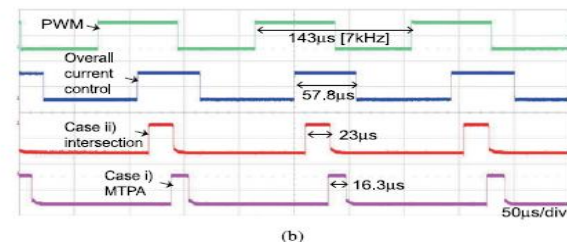
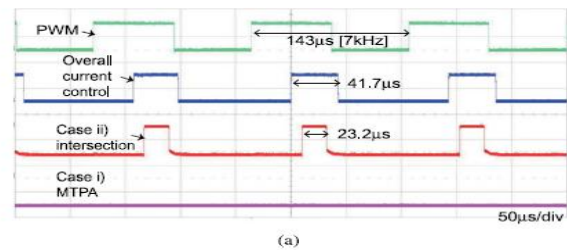
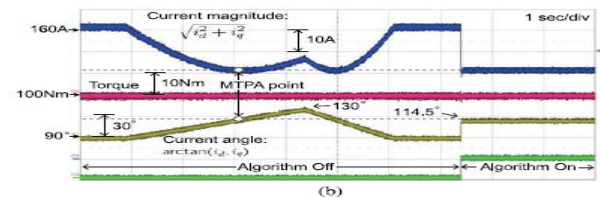
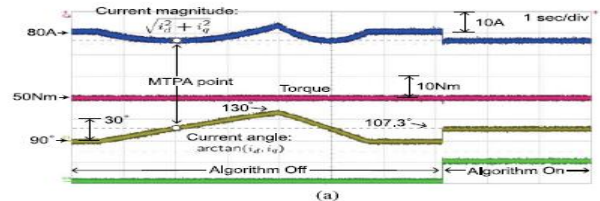
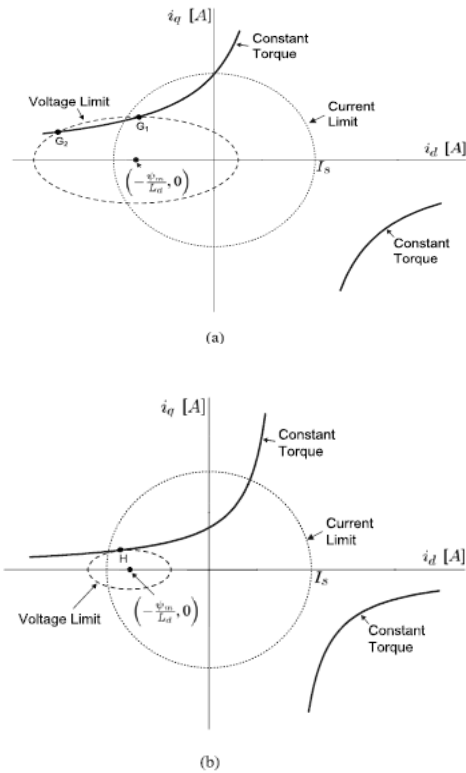


Fig. 5. Copper and iron loss of the IPMSM depending on mechanical speed and stator current: (a) 100 A. (b) 200 A.



Solving the necessary conditions simultaneously for  $i_d$ , we obtain the quartic polynomial

$$i_d^4 + A_1 i_d^3 + B_1 i_d^2 + C_1 i_d + D_1 = 0 \quad (16)$$

where  $A_1 = \frac{3\psi_m}{(L_d - L_q)}$ ,  $B_1 = \frac{3\psi_m^2}{(L_d - L_q)^2}$ ,  $C_1 = \frac{\psi_m^3}{(L_d - L_q)^3}$ , and  $D_1 = -\frac{16T_m^2}{9P^2(L_d - L_q)^2}$ .

#### IV. FERRARI'S SOLUTION TO QUARTIC EQUATIONS

In the above, two quartic polynomials are derived: from either the MTPA or the voltage limit. It is known that a general solution always exists for quartic polynomials. Lodovico Ferrari invented a systematic procedure to solve all quartics. In this section, analytic solutions are obtained utilizing Ferrari's method

A. Case i): (MTPA)

The general solution to (16) is given as [28]

$$i_d = -\frac{A_1}{4} \pm_s \frac{\eta_1}{2} \pm_t \frac{\mu_1}{2} \quad (18)$$

where

$$\alpha_1 = \frac{1}{3} (3A_1C_1 - 12D_1 - B_1^2) \quad (19)$$

$$\beta_1 = \frac{1}{27} (-2B_1^3 + 9A_1B_1C_1 + 72B_1D_1 - 27C_1^2 - 27A_1^2D_1) \quad (20)$$

$$\gamma_1 = \frac{B_1}{3} + \sqrt[3]{-\frac{\beta_1}{2} + \sqrt{\frac{\beta_1^2}{4} + \frac{\alpha_1^3}{27}}} + \sqrt[3]{-\frac{\beta_1}{2} - \sqrt{\frac{\beta_1^2}{4} + \frac{\alpha_1^3}{27}}} \quad (21)$$

$$\eta_1 = \sqrt{\frac{A_1^2}{4} - B_1 + \gamma_1} \quad (22)$$

$$\mu_1 = \sqrt{\frac{3}{4}A_1^2 - \eta_1^2 - 2B_1} \pm_s \frac{1}{4\eta_1} (4A_1B_1 - 8C_1 - A_1^3). \quad (23)$$

It should be noted that two  $\pm_s$  should have the same sign, while the sign of  $\pm_t$  is independent.

When  $r_1, r_2, r_3,$  and  $r_4$  are the solutions of a quartic polynomial, the discriminant is defined as

$$D = (r_1 - r_2)^2(r_1 - r_3)^2(r_1 - r_4)^2(r_2 - r_3)^2(r_2 - r_4)^2(r_3 - r_4)^2. \quad (24)$$

The discriminant tells us about the nature of its roots [29]. Noting that all of the coefficients of (16) are real,

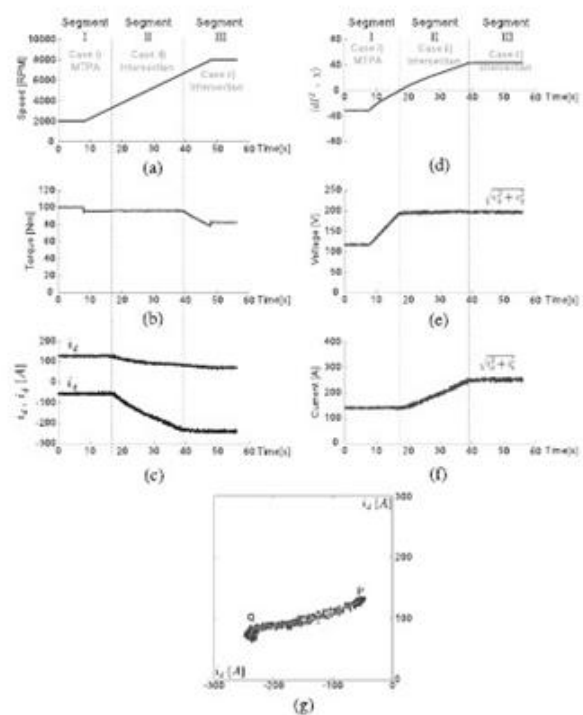
- if at least two of the roots coincide, then  $D = 0$ ;
- if all four roots are real or complex conjugates, then  $D > 0$ ;
- if two roots are real and two are complex conjugates, then  $D < 0$ .

For quartic polynomial (16), the discriminant is equal to [30]

$$\begin{aligned} D = & 256D_1^3 - 192A_1C_1D_1^2 - 128B_1^2D_1^2 + 144B_1C_1^2D_1 \\ & - 27C_1^4 + 144A_1^2B_1D_1^2 - 6A_1^2C_1^2D_1 - 80A_1B_1^2C_1D_1 \\ & + 18A_1B_1C_1^3 + 16B_1^4D_1 - 4B_1^3C_1^2 - 27A_1^4D_1^2 \\ & + 18A_1^3B_1C_1D_1 - 4A_1^3C_1^3 - 4A_1^2B_1^3D_1 + A_1^2B_1^2C_1^2. \end{aligned} \quad (25)$$

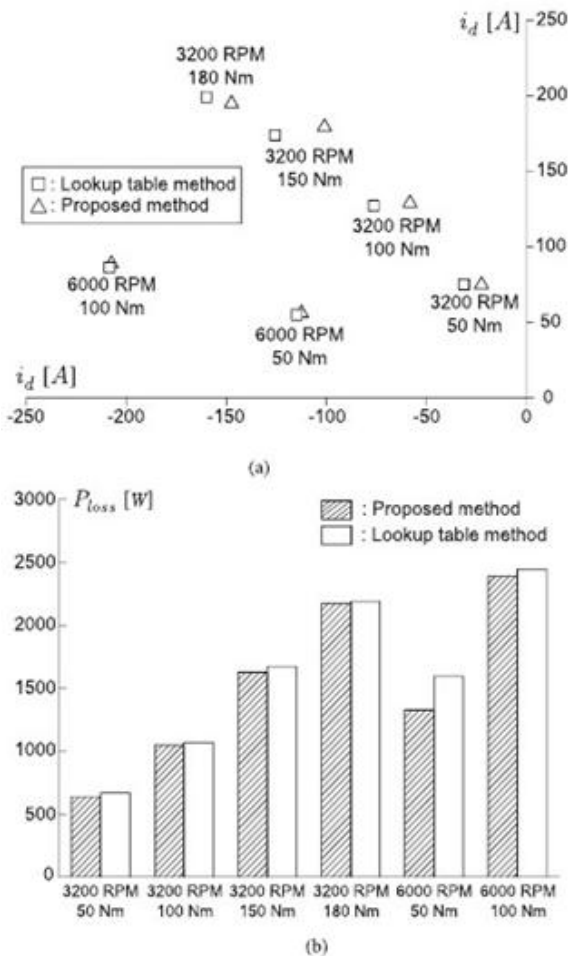
V. CONCLUSION FROM MTPA

The current minimizing solution is found on the intersection with the MTPA or a voltage limit, depending on the speed and torque. Thus, before calculating the solution, it is necessary to classify the cases. A method suggested here is to find a solution candidate from Case ii), and check whether it is the (sub) optimal solution or not. Specifically, for a given  $T_O$ , determine the intersection with the voltage limit. Then, find the location of the MTPA solution. If the MTPA solution is within the voltage limit, we need to use the MTPA solution. Otherwise, the pre calculated solution (Case ii)) is determined to be the desired one. Because testing is conducted before finding the MTPA solution, unnecessary calculation effort can be avoided. This *a priori* determining method is based on the local geometric analysis at the intersection  $N(id\beta, iq\beta)$ .



## REFERENCES

- [1] S. Morimoto, M. Sanada, and Y. Takeda, "Wide-speed operation of interior permanent magnet synchronous motors with high-performance current regulator," *IEEE Trans. Ind. Appl.*, vol. 30, no. 4, pp. 920–926, Jul./Aug. 1994.
- [2] S. Morimoto, M. Sanada, and Y. Takeda, "Effects and compensation of magnetic saturation in flux-weakening controlled permanent magnet synchronous motor drives," *IEEE Trans. Ind. Appl.*, vol. 30, no. 6, pp. 1632–1637, Nov./Dec. 1994.
- [3] G. H. Kang *et al.*, "Improved parameter modeling of interior permanent magnet synchronous motor based on finite element analysis," *IEEE Trans. Magn.*, vol. 36, no. 4, pp. 1867–1870, Jul. 2000.
- [4] B. Stumberger *et al.*, "Evaluation of saturation and cross-magnetization effects in interior permanent-magnet synchronous motor," *IEEE Trans. Ind. Appl.*, vol. 39, no. 5, pp. 1264–1271, Sep. 2003.
- [5] K. J. Meessen *et al.*, "Inductance calculations of permanent-magnet synchronous machines including flux change and self- and cross-saturations," *IEEE Trans. Magn.*, vol. 44, no. 10, pp. 2324–2331, Oct. 2008.
- [6] R. Nalepa and T. Orłowska-Kowalska, "Optimum trajectory control of the current vector of a nonsalient-pole PMSM in the field-weakening region," *IEEE Trans. Ind. Elec.*, vol. 59, no. 7, pp. 2867–2876, Jul. 2012.
- [7] G. Kang *et al.*, "A MTPA control scheme for an IPM synchronous motor considering magnet flux variation caused by temperature," in *Proc. IEEE APEC*, Feb. 2004, pp. 1617–1621.
- [8] R. Monajemy and R. Krishnan, "Implementation strategies for concurrent fluxweakening and torque control of the PMS synchronous motor," in *Proc. IEEE Ind. Appl. Society*, Oct. 1995, pp. 238–245.
- [9] Y. Jeong *et al.*, "Online minimum-copper-loss control of an interior permanent-magnet synchronous machine for automotive applications," *IEEE Trans. Ind. Appl.*, vol. 42, no. 5, pp. 1222–1229, Sep./Oct. 2006.
- [10] J. Lee *et al.*, "Loss-minimizing control of PMSM with the use of polynomial approximations," *IEEE Trans. Power Elec.*, vol. 24, no. 4, pp. 1071–1082, Apr. 2009.



## VI. CONCLUDING REMARKS

The current minimizing torque control method was considered for an IPMSM. In producing a desired torque, the current minimizing solution was sought. If the voltage limit was not active, it was possible to use the MTPA solution. Otherwise, it was necessary to use the intersection value between the voltage limit and torque curves. In both cases, quartic polynomials were induced, and Ferrari's method was used to obtain general solutions for all of the quartic polynomials.